Iranian Journal of Basic Medical Sciences
ijbms.mums.ac.ir

Cordycepin ameliorates ischemia/reperfusion-induced acute kidney injury via inhibiting apoptosis and necroptosis

Xiuzhao Fan [1, 2, 3#], Xiutao Han [4#], Zhibo Zhao [1, 2, 3], Junhu Li [1, 2, 3], Shuangshuang Tian [1, 2, 3], Fang Zhang [1, 2, 3], Xiaoshuang Zhou [1, 2, 3, 5, 6 c*]

[1] Department of Nephrology, Fifth Hospital of Shanxi Medical University, Taiyuan, Shanxi, 030012, China
[2] Department of Nephrology, Shanxi Provincial People's Hospital, Taiyuan, Shanxi, 030012, China
[3] Big Data Center of Kidney Disease, Shanxi Provincial People's Hospital, Taiyuan, Shanxi, 030012, China
[4] Department of Traditional Chinese Medicine, Yan'an Baota District People's Hospital, Yan'an, Shaanxi, 716000, China
[5] Shanxi Provincial Key Laboratory of Kidney Disease, Taiyuan, Shanxi, 030012, China
[6] Medicinal Basic Research Innovation Center of Chronic Kidney Disease, Ministry of Education, Shanxi Medical University, Taiyuan, Shanxi, 030012, China

ARTICLE INFO

Article type:
Original

Article history:
Received: Oct 20, 2025
Accepted: May 19, 2026

Keywords:
Acute kidney injury
Apoptosis
Cordycepin
Necroptosis
Receptor-Interacting Protein Serine-Threonine Kinase 1 (RIPK1)

ABSTRACT

Objective(s): Cordycepin (COR) is a natural bioactive compound derived from *Cordyceps militaris*. Relevant studies have shown that COR can alleviate kidney damage, but the underlying mechanism of its action in the treatment of acute kidney injury (AKI) remains to be further clarified.

Materials and Methods: The GSE148420 dataset and GeneCards were used to identify AKI-related targets. GeneCards was used to obtain ischemia/reperfusion (I/R)-related targets. BATMAN 1.0 and GeneCards were used to identify potential drug targets of COR. Renal function, tissue damage, and molecular markers were assessed to explore the effects of COR on apoptosis and necroptosis in the treatment of AKI.

Results: Network pharmacological analysis showed that AKI and COR shared 28 drug targets. Enrichment analysis showed that the targets were involved in signaling pathways, including apoptosis and necroptosis. *In vitro* experiments revealed that COR alleviated hypoxia/re-oxygenation(H/R)-induced HK-2 cells injury by reducing the expression of Bax and cleaved-Caspase3 while increasing the expression of Bcl-2. Necroptosis was lessened under COR treatment *in vitro* and in H/R-induced HK-2 cells by reducing the expression of RIPK1, RIPK3, MLKL, and p-MLKL. COR and Nec-1 (a RIPK1 inhibitor) had the same inhibitory effect, confirming the role of COR in alleviating AKI by inhibiting RIPK1-driven necroptosis. COR alleviated AKI by ameliorating renal morphology injury and pathological injury *in vivo*, manifested as a decrease in Scr and BUN levels, a significant reduction in the mRNA expression levels of *KIM-1* and NGAL, and a decrease in p-MLKL at the immunohistochemical level.

Conclusion: COR may ameliorate I/R-induced AKI by inhibiting apoptosis and RIPK1/RIPK3/p-MLKL-mediated necroptosis.

▶ Please cite this article as:
Fan X, Han X, Zhao Zh, Li J, Tian Sh, Zhang F, Zhou X. Cordycepin ameliorates ischemia/reperfusion-induced acute kidney injury via inhibiting apoptosis and necroptosis. Iran J Basic Med Sci 2026; 29:

Introduction

Acute kidney injury (AKI) is a clinical syndrome characterized by a sudden decline in glomerular filtration rate, rapid elevation of serum creatinine, and/or reduced urine output (1, 2). The mortality rate among hospitalized adult AKI patients in China ranges from 14% to 60% (3). AKI often progresses to chronic kidney disease and is a major risk factor for end-stage renal disease (4-6). However, effective targeted pharmacological treatments for AKI remain scarce in clinical practice. AKI can be triggered by various factors, including drug toxicity, ischemia/reperfusion (I/R) injury, mechanical trauma, inflammation, and oxidative stress (7, 8). Among these, I/R injury is widely recognized as one of the most common causes of AKI (9).

Apoptosis, a tightly regulated cell death process critical to biological homeostasis, is a primary contributor to renal dysfunction in AKI (10). Under normal conditions, apoptosis is precisely controlled to maintain physiological balance. However, during AKI, this regulatory mechanism may become imbalanced, leading to excessive renal cell apoptosis and subsequent decline in renal function (11). Consequently, strategies targeting apoptotic pathways have been extensively explored for AKI treatment. Yet effective anti-apoptotic interventions remain absent in clinical settings, likely due to the complexity of cell death mechanisms. Recent advances suggest that other forms of cell death, including necroptosis, ferroptosis, and pyroptosis, also play significant roles in AKI pathogenesis (12-15). However, the specific mechanisms of necroptosis and the relationship with AKI remain unclear, warranting

***Corresponding author:** Xiaoshuang Zhou. Department of Nephrology, Fifth Hospital of Shanxi Medical University, Taiyuan, Shanxi, 030012, China. Tel/ Fax: +86-13466821865, Email: xiaoshuangzhou69@163.com
# These authors contributed equally to this work

further investigation.

Necroptosis, a form of programmed cell death, differs from apoptosis in that necroptotic cells exhibit membrane rupture—a hallmark of necrosis (16). Necroptosis is mediated by receptor-interacting protein kinase 1 (RIPK1), RIPK3, and mixed lineage kinase domain-like protein (MLKL) and is implicated in atherosclerosis, I/R injury, sepsis, and neurodegenerative diseases (17). Recent studies demonstrate that inhibitors targeting necroptosis-related proteins or genetic knockout of these proteins can mitigate renal I/R injury (18), suggesting that modulating necroptosis may be a therapeutic strategy for I/R-induced AKI.

Traditional Chinese medicine is widely used to treat a variety of renal diseases, including AKI, as well as their complications (19-22). *Cordyceps militaris* is an ascomycete that is valued for its medicinal and nutritional properties. It has been widely used in Asia for centuries, both as a dietary supplement and in pharmaceutical applications (23). *C. militaris* mycelia powder and capsules are commercial products marketed for lung nourishment, kidney invigoration, and the treatment of conditions such as cough, asthma, and phlegm, among other health concerns(24, 25). *C. militaris* exhibits a range of clinical health effects, including immunomodulatory, anticancer, antioxidant, anti-inflammatory, and antimicrobial activities (26, 27). Yu *et al*. demonstrated that *C. militaris* treatment alleviated renal injury in type 2 diabetic nephropathy mice (28). Yang *et al*. reported that *C. militaris* mycelial therapy may prevent renal function deterioration in mice with chronic kidney disease (29). *Cordycepin* (COR), a representative bioactive component of *C. militaris* (30), is an adenosine analog with antioxidant, immunomodulatory, hypolipidemic, anti-inflammatory, anticancer, and antibacterial properties. Low-dose COR can alleviate renal IRI (31). COR can inhibit kidney injury and tissue inflammation during IRI by inhibiting NF-kappa B-mediated pyroptosis (32). It can inhibit apoptosis and renal fibrosis and rescue autophagy, thus alleviating kidney damage in diabetic nephropathy (33-36). According to Q. Chen *et al*., COR alleviates renal IRI by suppressing the p38/JNK signaling pathway in renal tubular epithelial cells, thereby attenuating inflammatory responses, apoptosis, and ferroptosis (37). In a murine model of unilateral ureteral obstruction-induced renal interstitial fibrosis, COR was reported to interfere with pro-fibrotic Smad signaling, suggesting its potential for treating fibrotic diseases (38). However, whether COR modulates apoptosis and necroptosis to ameliorate renal I/R injury remains unclear.

This study is based on network pharmacology to explore targets and potential mechanisms of COR in the treatment of AKI. Furthermore, *in vivo* experiments using a mouse renal I/R model and *in vitro* experiments using an H/R-induced HK-2 cell model were conducted to validate the effects of COR on apoptosis and necroptosis in AKI and to explore their underlying mechanisms. The findings aim to provide clinical evidence for the application of COR and serve as a reference for the prevention and treatment of I/R-induced AKI.

Materials and Methods

Bioinformatics analysis

Using "Acute Kidney Injury and ischemia reperfusion" as the keyword, the gene expression profile of the GSE148420 dataset and its matched official platform annotation file (accession number: GPL14746-13667) were retrieved from the NCBI GEO database, comprising 3 days after I/R-induced kidney injury tissues (n=4, GSM4469955, GSM4469956, GSM4469957, GSM4469958) and sham-operated kidney tissues (n=4, GSM4469951, GSM4469952, GSM4469953, GSM4469954). Perform standardization processing on the gene expression profile. Probes mapped to multiple genes and probes without official gene symbol annotation were fully removed. For multiple probes uniquely mapped to the same gene, the mean expression value was calculated as the final expression level of the gene. The R package "Limma" was employed to identify differentially expressed genes (DEGs) with a significance threshold of $|logFC| > 0.5$ & adj. P. Val < 0.05. Targets related to "Acute Kidney Injury" and "ischemia reperfusion" were obtained from GeneCards (https://www.genecards.org), while COR targets were additionally acquired from GeneCards and the BATMAN 1.0 database (http://bionet.ncpsb.org.cn/batman-tcm/index.php/Home/Index/index). The R package "corrplot" and Pearson correlation analysis were used to assess correlations among drug targets. The R package "clusterProfiler" was utilized for GO functional annotation and KEGG pathway enrichment analysis of drug targets, with a significance threshold of $P < 0.05$. All parameter details, original data, and enrichment results are provided in Supplementary Materials 1, 2, and 3, respectively.

Cell culture and experimental protocol

Human renal cortex proximal tubule epithelial cells (HK-2) were purchased from Pnocel Life Science Co., LTD. (Wuhan, China). HK-2 cells were routinely cultured in a cell incubator at 37 ˚C, 5% CO2, and 95% air using MEM medium (Cat. No. PYG0029, Boster, China) supplemented with 10% fetal bovine serum and 1% penicillin-streptomycin-gentamicin mixed solution (Cat. No. P1410, Solarbio, China). COR was purchased from MedChemExpress (Cat. No. HY-N0262, MCE, USA). COR was dissolved in sterile dimethyl sulfoxide (DMSO) to prepare a stock solution, which was then diluted to the working concentration with sterile normal saline before administration, with a final DMSO concentration of ≤0.1% in the working solution.

To establish the H/R model, the serum-free medium was first replaced with sugar-free DMEM medium (Cat. No. PM150446, Procell, China), which was cultured in an anoxic incubator (94% N_2, 5% CO_2, and 1% O_2) for 24 hr, and then the complete medium was replaced and cultured in a cell incubator at 37 ˚C and 5% CO_2 for 3 hr.

To verify the role of necroptosis in the effect of COR on H/R-induced AKI, HK-2 cells were divided into six groups: (1) Normal control group (CTL): cells were cultured in a conventional cell incubator (95% air and 5% CO_2) with complete medium throughout the process; (2) COR group: one day before H/R modeling, cells were pretreated with COR (20μmol/L) and then cultured in complete medium in a conventional cell incubator; (3) Nec-1 group: cells were pretreated with Nec-1 (50μmol/ml, Cat. No. HY-15760, MCE, USA) at the same time and then cultured in complete medium in a normoxic incubator; (4) H/R group: cells in the H/R group were treated with PBS (Cat. No. MA0015, Meilun, China) one day before H/R, followed by 24 hr of hypoxia and 3 hr of reoxygenation; (5) H/R+COR group: one day before H/R, cells in the H/R+COR group were

pretreated with COR (20μmol/l) and then subjected to 24 hr of hypoxia and 3 hr of reoxygenation; (6) H/R+Nec-1 group: one day before H/R, cells in the H/R+Nec-1 group were pretreated with Nec-1 (50 μmol/ml) and then subjected to 24 hr of hypoxia and 3 hr of reoxygenation.

Animals and experimental protocols

Eighteen 8-week-old C57BL/6J mice were procured from Beijing Huafukang Biotechnology Co., Ltd. (SPF grade) and housed in the Laboratory Animal Center of Shanxi Provincial People's Hospital under specific pathogen-free (SPF) conditions. All mice were housed six per cage on a 12-hour light/dark cycle and in a climate-controlled environment, and had free access to food and water. To guarantee uniformity, the environmental temperature was sustained at 25 ˚C, and the relative humidity was regulated between 40% and 50%.

The construction of the I/R model requires that the experimental mice be fasted for 12 hr in advance. Before the operation, the mice are weighed and anesthetized with 1% pentobarbital sodium at a dose of 0.05 mg/g by intraperitoneal injection. After making parallel incisions on both sides of the spine on the back, the kidneys are fully exposed. The bilateral renal pedicles are clamped with arterial clamps to cause ischemia for 45 min. We can observe that the kidneys turn purple-black within 1-2 min after clamping the renal pedicles, indicating successful ischemia. After 45 min, the clamps are removed, and the kidneys change from purple-black to bright red, regaining their original color, indicating successful reperfusion. At the end of the operation, the bilateral kidneys are returned to their original positions, and the wounds are sutured layer by layer. During surgery, animals are placed on a heating pad to prevent hypothermia. Postoperative analgesia is administered to relieve pain and minimize distress.

To determine whether COR has a protective effect on I/R-induced AKI, 18 healthy male C57BL/6 mice were randomly divided into three groups of six mice each using a random number table: sham operation group (Sham), I/R, I/R+DMSO, and I/R+COR group. (1) In the Sham group, mice received the same volume of normal saline by intraperitoneal injection for one week, and only the kidneys were exposed without ischemia treatment; (2) In the I/R group, mice received the same volume of normal saline by intraperitoneal injection for one week before the I/R-induced AKI model was established; (3) In the I/R+COR group, mice received COR (10 mg/kg) by intraperitoneal injection for one week before the I/R-induced AKI model was established. At the conclusion of the experiment, all animals were deeply anesthetized with isoflurane to ensure complete loss of consciousness. Euthanasia was then performed promptly by cervical dislocation, carried out by trained personnel in accordance with humane endpoints.

CCK8

Firstly, we conducted cytotoxicity tests on COR using the CCK8 method. Normal-growing HK-2 cells were collected and seeded into blank, control, and experimental wells. No cells were inoculated in the blank wells; only complete culture medium was added. In the control wells, cells were inoculated and cultured until the end of the experiment. In the experimental wells, cells were cultured in complete culture medium for 12 hr, after which the medium was replaced with serum-free MEM for another 12 hr. Different concentrations of COR (0, 10, 20, 40, 80 **μ**mol/L) were added, and the cells were treated for 24 hr. Then, 10**μ**l of CCK8 solution (Cat. No. SC119-02, Sevensea Innovation, China) and 90**μ**l of serum-free medium were added to each well, and the plates were incubated in a 37 ˚C incubator for 0.5 to 4 hr. Starting from 0.5 hr, the OD value was detected at 450 nm until the absorbance value of the control well was around 1.0, at which point the detection was stopped.

Secondly, we used the CCK8 assay to assess the effect of COR on H/R cell viability. HK-2 cells were seeded in 96-well plates at a density of 6×10^3 cells/well in both experimental and control wells. The blank wells contained only the culture medium without cells. The HK-2 cells in both the control and experimental wells were cultured in complete medium for 12 hr and then switched to serum-free medium for another 12 hr. The experimental wells were treated with COR at concentrations of 0, 10, 20, 40, and 80 **μmol**/L for 24 hr, followed by 24 hr of hypoxia and 3 hr of reoxygenation. Control wells were switched to complete medium and placed in a conventional cell culture incubator. 10**μ**l of CCK8 solution was added to each well, and the plates were incubated at 37 ˚C for 0.5 to 4 hr. The OD value was then measured. The calculation formula is as follows: cell survival rate = [(experimental well - blank well) / (control well - blank well)] × 100%.

Cell immunofluorescence

HK-2 was inoculated onto cell slides in 24-well plates at 3×10^4 cells per well. After different treatments according to the experimental groups, immunofluorescence staining was performed. The treated cell slides were washed three times with PBS, fixed with 4% paraformaldehyde for 15 min, permeabilized with 0.5% TritonX-100 at room temperature for 20 min, washed three times with PBST, blocked with 3% BSA at room temperature for 30 min, and then diluted phosphorylated MLKL (p-MLKL) antibody at a ratio of 1:100 and appropriately added to each slide. The slides were placed in a humid box and incubated at 37 ˚C overnight. The next day, the slides were incubated with fluorescently labeled secondary antibodies (1:20) at 37 ˚C in the dark for 1 hour, followed by DAPI incubation in the dark for 5 min, and then sealed with mounting medium containing an anti-fluorescence quenching agent. Fluorescence images were captured using a fluorescence microscope.

Western blotting

HK-2 cells were lysed using the RIPA lysis buffer, and total cellular proteins were extracted. Protein concentration was determined using the BCA protein assay kit. 50 **μg** of protein samples were run on 10% or 12% SDS-PAGE gels and then transferred onto polyvinylidene fluoride membranes. The membranes were then incubated in 5% skimmed milk at room temperature for 1 hr to block. After blocking, the membranes were washed 3 times with TBST for 10 min each, then primary antibodies were added and incubated at 4 ˚C overnight. The membranes were recovered the next day and incubated with horseradish peroxidase-conjugated secondary antibodies. After washing with TBST 3 times, ECL staining solution was added, and the gel was imaged using the Bio-Rad gel imaging system. β-actin was used as the unified internal reference for all blots. Semi-quantitative analysis of target proteins was performed using

ImageJ, with consistent normalization of the target band gray value to the corresponding β-actin level in the same lane across all assays.

The primary antibodies used in this study were β-actin (Cat. No. AC026, ABclonal, China), RIPK1 (Cat. No. WL04522, Wanlei Biotechnology, China), RIPK3 (Cat. No. 17563-1-AP, Proteintech, China), MLKL (Cat. No. ET1601-25, HuaAn Biotechnology, China), phospho-MLKL (p-MLKL, Cat. No. 91689, CST, USA), Bax (Cat. No. T40051, Abmart, China), Bcl-2 (Cat. No. T40056, Abmart, China), Caspase3 (Cat. No. T40044, Abmart, China), and Cleaved Caspase3 (Cat. No. WL02117, Wanlei Biotechnology, China).

Renal function

After collecting mouse serum, blood urea nitrogen (BUN) and serum creatinine (Scr) levels were quantified using a commercially available kit (Nanjing Jiancheng Bioengineering Institute, China).

Hematoxylin-eosin staining

The renal tissues were fixed with 4% paraformaldehyde and then embedded in paraffin before sectioning. Renal tissues were serially sectioned to a uniform thickness of 5 μm for subsequent Hematoxylin-Eosin (HE) staining, immunohistochemistry (IHC), and immunofluorescence (IF) assays. The subsequent sections were stained with HE staining. The samples were evaluated using the tubule injury score, and the degree of renal tubule tissue injury was assessed with a semi-quantitative scoring system. Observers randomly selected 10 fields of view under a high-power microscope (400X) and performed the tubule injury scoring. According to the conditions of renal tubule dilation, tubule casts formation, brush border shedding, epithelial cell shedding and necrosis, granular degeneration, vacuolar degeneration, nuclear pyknosis, and inflammatory cell infiltration, the percentage of injured renal tubules was calculated. The scoring criteria were as follows: 0 points: no injury; 1 point: tubule injury < 10%; 2 points: tubule injury 10%-25%; 3 points: tubule injury 26%-45%; 4 points: tubule injury 46%-75%; 5 points: tubule injury > 75%.

Immunofluorescence

For quantitative analysis of immunofluorescence staining, all images were captured using consistent confocal microscope settings. The mean fluorescence intensity (MFI) of the target protein was quantified with ImageJ.

RNA extraction and real-time fluorescence quantitative PCR analysis

Total RNA was extracted from kidney tissue using a Total RNA Extraction Kit (Mei5 Biotechnology, Beijing, China). The RNA concentration and purity were quantified using a NanoDrop ultraviolet spectrophotometer. Subsequently, the RNA was reverse-transcribed into cDNA using a cDNA Reverse Transcription Kit (Mei5 Biotechnology, Beijing, China). Real-time fluorescence quantitative PCR was performed using a SYBR Green PCR Kit (Mei5 Biotechnology, Beijing, China) on a Bio-Rad CFX96 Real-Time PCR Detection System (Bio-Rad, USA). The relative expression levels of genes were calculated using the 2^-△△CT method. Data analysis was conducted using Microsoft Excel and GraphPad Prism 9. All primers were designed using the professional online primer design platform on the official website of Sangon Biotech (Shanghai, Co., Ltd.) (https://www.sangon.com/index), with strict compliance with MIQE guidelines. The primer sequences are listed in Table 1.

Transmission electron microscope

Kidney tissues or HK-2 cell aggregates were collected and fixed with 2.5% glutaraldehyde. Following PBS rinsing, the fixed samples were sequentially dehydrated with a graded ethanol series and subsequently embedded for ultrathin sectioning. The sections were stained with 1% osmium tetroxide solution for 1 hr, followed by staining with 2% uranyl acetate solution for 30 min. Finally, the sections were examined using an HT-7500 transmission electron microscope (TEM).

Statistical analysis

The statistical analysis of drug concentration and drug toxicity was conducted using the T-test in R software. Other experimental data were analyzed using GraphPad Prism 9.0. Biological replicates were defined as the basis for sample size: n=3 independent biological replicates for all *in vitro* experiments, and n=6 mice per group for *in vivo* experiments. An unpaired two-tailed Student's t-test was used for two-group comparisons, while one-way analysis of variance (ANOVA) followed by Tukey's multiple comparison test was used for comparisons among multiple groups. Statistical significance was defined as $P<0.05$, with the following notations: $^{*}P<0.05$, $^{**}P<0.01$, $^{***}P<0.001$, $^{****}P<0.0001$, and $^{ns}P>0.05$.

Results

Bioinformatics analysis of drug targets for I/R-induced AKI and COR

In this study, sequencing data from GSE148420 were obtained for samples collected 3 days after I/R and sham-operated controls. Principal Component Analysis (PCA) revealed distinct clustering between the two groups (shown in Figure 1A), identifying 7,540 DEGs. Using GeneCards, 11,630 AKI-related targets and 1,725 I/R-related targets were identified. The BATMAN 1.0 and GeneCards databases provided 82 and 85 COR-related genes, respectively. The union of these datasets yielded 162 COR-related genes. Ultimately, 28 shared drug targets were identified across I/R-induced AKI and COR (as shown in Figure 1B), and their expression levels are shown in Figures 1C and D. The correlations among these drug targets are shown in Figure 1E.

GO functional annotation indicated that drug targets are involved in biological processes such as regulation of apoptotic signaling pathways, hypoxia response, and

Table 1. Primer sequence used for real-time PCR

Primer	Forward primer (5'→3')	Reverse primer (5'→3')
KIM-1	CTGCTGCTACTGCTCCTTGTG	CACGCTTAGAGATGCTGACTTCC
NGAL	ACCACGGACTACAACCAGTTCG	CTTGGCAAAGCGGGTGAAACG
β-actin	GTGCTATGTTGCTCTAGACTTCG	ATGCCACAGGATTCCATACC

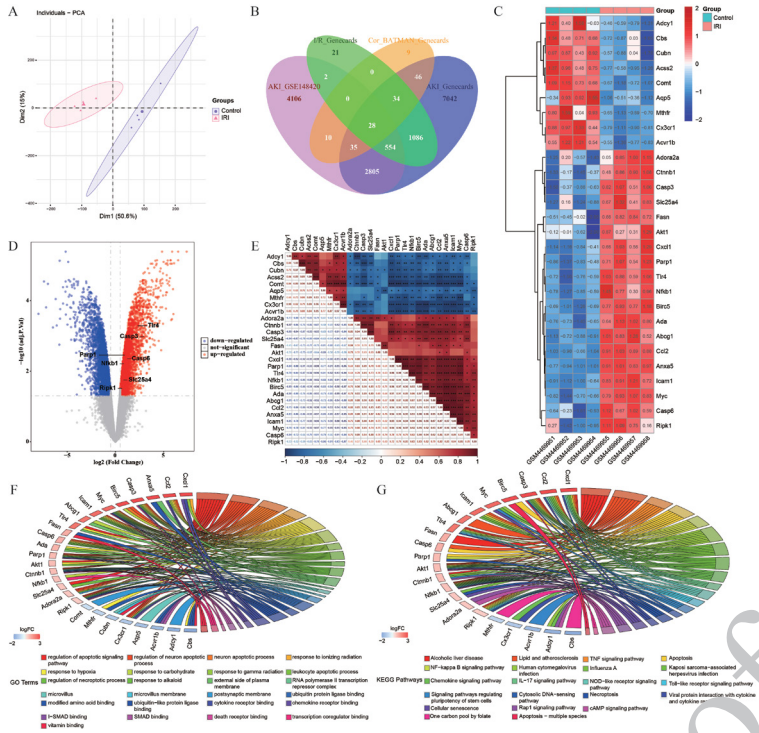

Figure 1. Mechanistic analysis of drug targets among I/R, AKI, and COR
(A) Principal Component Analysis of GSE148420. (B) Screen the common drug targets of I/R, AKI, and COR. (C) Heatmap of 28 drug targets. (D) Volcano plot of 28 drug targets. (E) The correlation of drug targets. (F) The top 10 chord plot of each category of GO enrichment. (G) The top 5 chord plot of each category of KEGG pathways
I/R: Ischemia/reperfusion; AKI: Acute kidney injury; COR: Cordycepin

modulation of necroptosis (shown in Figure 1F). KEGG Pathway Enrichment Analysis revealed that these drug targets participate in pathways including TNF signaling, apoptosis, NF-kappa B signaling, necroptosis, NOD-like receptor signaling, and Toll-like receptor signaling (shown in Figure 1G).

COR mitigates H/R-induced apoptosis in HK-2 cells

HK-2 cells were incubated with 0, 10, 20, 40, and 80 μmol/l COR for 24 hr, and then the CCK8 assay was performed to assess COR toxicity. The results show that COR has no obvious toxicity when the concentration is 10-80μmol/L (shown in Figure 2A). HK-2 cells were pretreated with COR at 0, 10, 20, 40, and 80 for 24 hr, and then the H/R model was established. The CCK8 assay results showed that H/R could significantly down regulate the activity of HK-2 cells. When the concentration of COR was 20μmol/L, the protective effect on H/R-induced HK-2 cells injury was the most significant (shown in Figure 2B). Therefore, a drug concentration of 20 μmol/L was used for intervention in subsequent experiments.

TEM results showed normal morphology in the control group, whereas H/R-induced HK-2 cells exhibited typical necroptotic features, including increased permeability, plasma membrane rupture, and organelle loss. However, COR pretreatment significantly alleviated these injuries (shown in Figure 2C).

Compared to the control group, H/R-treated HK-2 cells showed increased expression of apoptosis-related proteins Bax and cleaved-Caspase3, along with decreased Bcl-2 expression. COR pretreatment reversed these changes in protein expression. The result indicates that COR effectively mitigates H/R-induced apoptosis in HK-2 cells (as shown in Figures 2D and 2E).

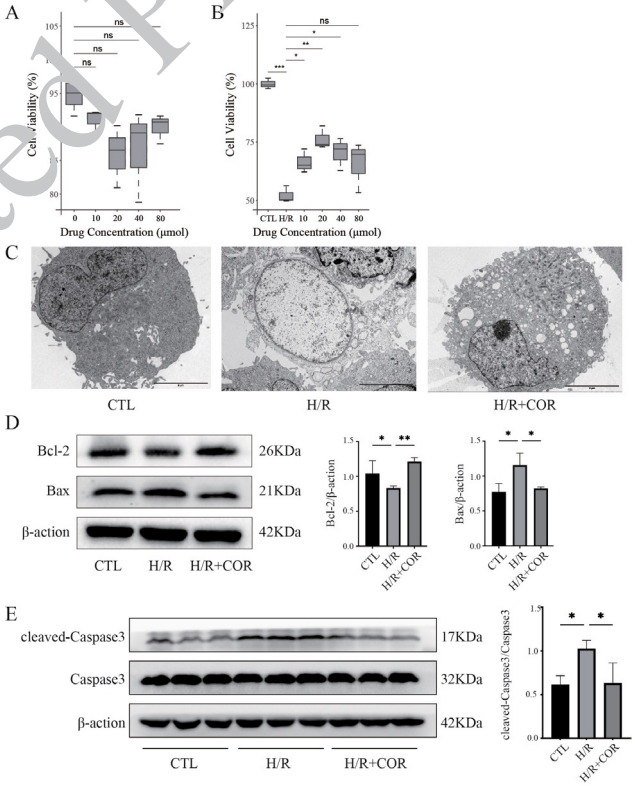

Figure 2. Effect of COR on apoptosis in mouse H/R-induced HK-2 cells
(A) Drug toxicity evaluation of gradient concentrations of COR in HK-2 cells, detected by CCK-8 assay (n=3). (B) Effect of gradient concentrations of COR on the viability of H/R-injured HK-2 cells, detected by CCK-8 assay (n=3). Data were analyzed using an unpaired two-tailed Student's t-test. (C) TEM images of HK-2 cells in each group. Magnification: 2.5K. (D, E) Western blotting analysis of Bcl-2, Bax, cleaved-Caspase3, and Caspase3 in each group (n=3). Data were analyzed using one-way ANOVA with Tukey's test and expressed as the means±SD. $^{ns}P>0.05$, $^{*}P<0.05$, $^{**}P<0.01$, $^{***}P<0.001$
COR: Cordycepin; H/R: Hypoxia/re-oxygenation

Effect of COR on necroptosis in H/R-induced HK-2 cells

Western blotting demonstrated that the H/R group significantly up-regulated necroptosis-related proteins RIPK1, RIPK3, MLKL, and p-MLKL compared to the control group. COR pretreatment notably reduced the expression levels of these proteins (shown in Figure 3A). Immunofluorescence staining further confirmed that COR pretreatment significantly reduced p-MLKL fluorescence intensity in H/R-induced HK-2 cells, indicating its inhibitory effect on necroptosis (as shown in Figure 3C).

To investigate whether COR inhibits necroptosis via RIPK1, RIPK1 expression was suppressed using Nec-1. Both COR and Nec-1 similarly inhibited RIPK1, RIPK3, MLKL, and p-MLKL expression in H/R-induced HK-2 cells (shown in Figure 3B). This suggests that COR likely suppresses H/R-induced necroptosis by modulating the RIPK1/RIPK3/p-MLKL signaling pathway.

COR ameliorates I/R-induced AKI

To evaluate the protective role of COR in mice with I/R-induced AKI, mice were divided into Sham, I/R, I/R+DMSO, and I/R+COR groups. Schematic timeline of COR prophylactic pre-treatment and I/R surgery is shown in Figure 4A. Serum renal function markers were measured using assay kits. Compared to the Sham group, the I/R group exhibited significantly elevated serum creatinine (Scr) and blood urea nitrogen (BUN) levels. However, COR treatment significantly reduced these indicators compared with the I/R group (as shown in Figure 4B). Compared to the I/R group, the I/R +DMSO group had no significant effect on

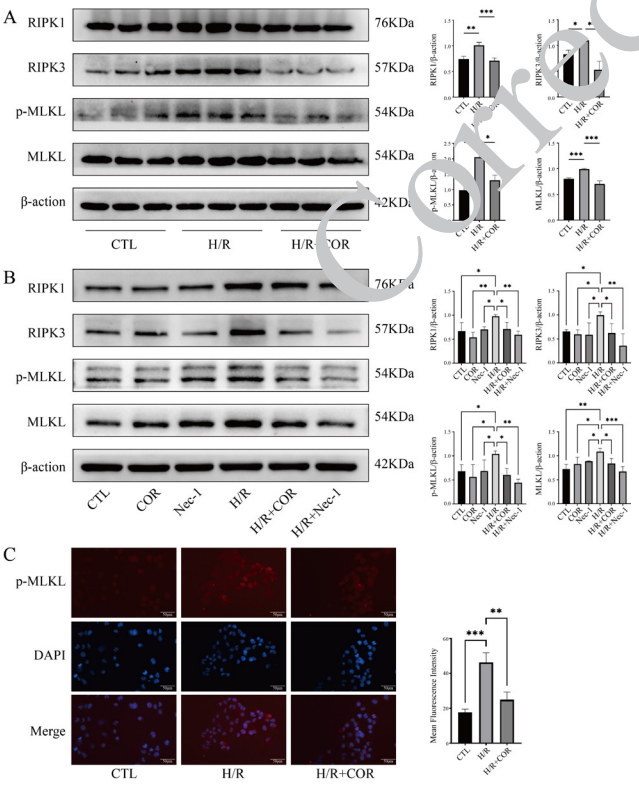

Figure 3. Effect of COR on necroptosis in mouse H/R-induced HK-2 cells (A, B) Western blotting analysis of RIPK1, RIPK3, p-MLKL, and MLKL in HK-2 cells from each group (n=3). (C) Quantitative analysis of the mean fluorescence intensity of p-MLKL (n=3). Magnification: 40X. Data were analyzed using one-way ANOVA with Tukey's test and expressed as the means±SD. $^{ns}P>0.05$, $^{*}P<0.05$, $^{**}P<0.01$, $^{***}P<0.001$
COR: Cordycepin; H/R: Hypoxia/re-oxygenation

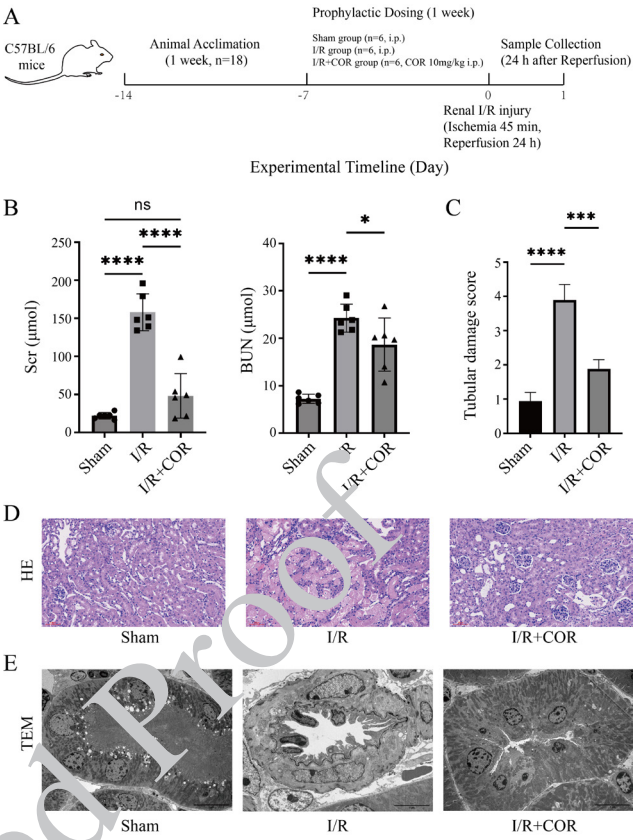

Figure 4. Effect of COR treatment on renal function and pathological injury in I/R-induced AKI mice
(A) Schematic timeline of the *in vivo* experimental protocol. (B) Levels of serum creatinine (Scr) and blood urea nitrogen (BUN) in each group (n=6). (C) Renal tubular damage scores of renal tissues in each group (n=6). (D) HE staining of renal tissues in each group (n=6). Magnification: 20X. (E) TEM manifestations of renal tubular in each group (n=6). Magnification: 1.5K. Data were analyzed using one-way ANOVA with Tukey's test and expressed as the means±SD. $^{ns}P>0.05$, $^{*}P<0.05$, $^{**}P<0.01$, $^{***}P<0.001$
COR: Cordycepin; I/R: Ischemia/reperfusion; AKI: Acute kidney injury

renal function, completely excluding the non-specific effect of the solvent (Supplementary Figure 1A).

Histopathological analysis via HE staining revealed severe tubular injuries in the I/R group, including tubular epithelial cell detachment, brush border loss, exposed basement membranes, nuclear pyknosis, tubular dilation, and cast formation. These injuries were markedly attenuated in the I/R+COR group (shown in Figure 4D). Semiquantitative tubular injury scores (shown in Figure 4C) confirmed that the I/R group had significantly more serious damage than the Sham group ($P<0.0001$), while the I/R+COR group showed reduced damage compared to the I/R group ($P<0.001$). TEM observations aligned with H&E results, showing tubular dilation and epithelial cell loss in the I/R group and notable improvement in the COR-pretreated group (shown in Figure 4E).

COR protects against I/R-induced AKI by reducing renal injury and necroptosis

Compared to the sham group, I/R-treated mice exhibited significantly increased mRNA expression of kidney injury molecule-1 (*KIM-1*) and neutrophil gelatinase-associated lipocalin (*NGAL*). COR pretreatment significantly downregulated these markers compared with the I/R group (shown in Figure 5A).

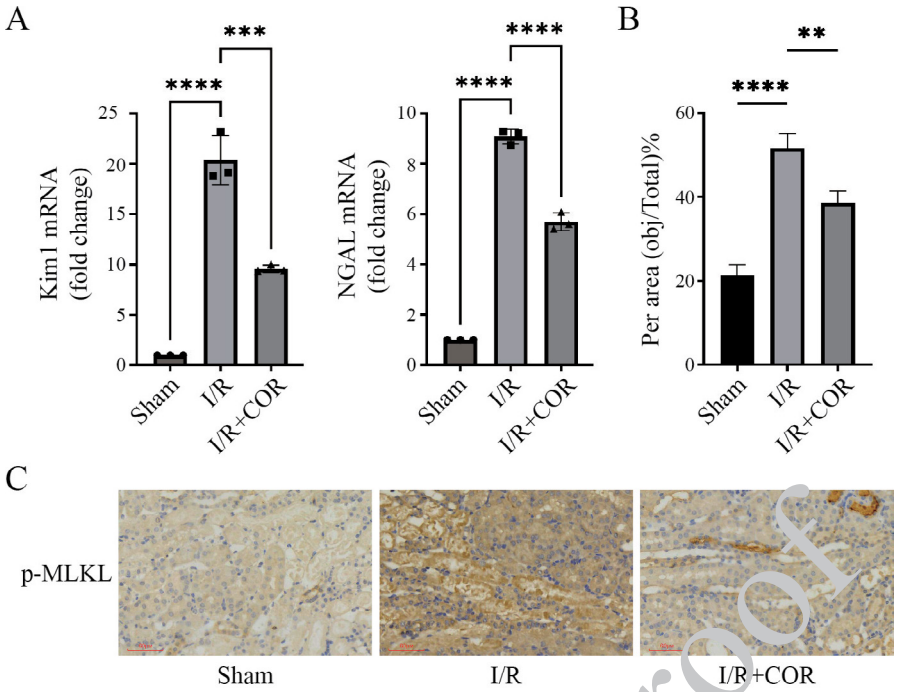

Figure 5. Effect of COR on renal injury and necroptosis-associated molecules in I/R-induced AKI mice
(A) Relative mRNA expression of renal injury markers KIM-1 and NGAL in renal tissues of each group (n=6). (B, C) Representative Immunohistochemical staining images of p-MLKL in mouse renal tissues (n=6). Magnification: 20X. Data were analyzed using one-way ANOVA with Tukey's test and expressed as the means±SD. $^{ns}P>0.05$, $^{*}P<0.05$, $^{**}P<0.01$,$^{***}P<0.001$
COR: Cordycepin; I/R: Ischemia/reperfusion; AKI: Acute kidney injury

Immunohistochemical staining for p-MLKL in renal tissues showed significantly up-regulated p-MLKL expression in the I/R group compared to the Sham group. COR pretreatment reduced p-MLKL expression in the I/R+COR group, further supporting its inhibitory effect on necroptosis (shown in Figure 5B, C).

Discussion

AKI is a complex pathophysiological response involving oxidative stress accumulation, inflammatory reactions, renal tubular cell damage, and endothelial microvascular dysfunction, all of which influence the extent of tubular injury (39-45). Extensive studies have suggested that substantial AKI progresses to chronic kidney disease (46-50). I/R-induced AKI triggers various forms of renal tubular epithelial cell death, including apoptosis, necrosis, ferroptosis, pyroptosis, and necroptosis (9, 13, 15, 51, 52). Due to its intricate pathophysiology, effective clinical strategies for prevention and treatment remain limited.

TCM has been utilized to treat various diseases, including renal injury (53, 54), liver damage (55, 56), cardiovascular diseases (57-59), and cerebrovascular disorders (60). Renal I/R injury can cause interactions among tubular epithelial cell damage, endothelial dysfunction, and inflammation, ultimately leading to renal tissue injury (61). TCM monomers such as COR, tanshinone, paeoniflorin, berberine, poricoic acid A, ligustrazine, and erythro-guaiacylglycerol-β-ferulic acid ether have demonstrated protective effects against renal damage, including I/R injury (62-64). COR has been shown to reduce inflammatory cell infiltration, inhibit extracellular matrix accumulation, and immune complex deposition in renal interstitium, thus protecting the renal tissue (38, 65). Experimental studies in animal models reveal that COR significantly lowers serum creatinine and urea nitrogen levels, thereby alleviating renal I/R injury (66, 67). In our study, network pharmacology identified 28 shared drug targets between I/R-induced AKI and COR, including Ripk1, Casp3, Akt1, Icam1, Nfkb1, Ccl2, Anxa5, Birc5, Abcg1, Myc, Cxcl1, Tlr4, Acss2, Cx3cr1, Acvr1b, Ada, Parp1, Casp6, Cbs, Adcy1, Ctnnb1, Mthfr, Cubn, Aqp5, Comt, Fasn, Slc25a4, and Adora2a. GO functional annotation indicated that targets participate in biological processes such as apoptotic signaling regulation, hypoxia response, and necroptosis modulation. KEGG pathway enrichment highlighted their involvement in apoptosis, necroptosis, and NF-kappa B signaling pathways.

Apoptosis, a programmed cell death mechanism, occurs through intrinsic (mitochondrial), extrinsic (death receptor), or cross-talk pathways (68, 69). In the intrinsic pathway, cellular stress enhances mitochondrial outer membrane permeability via Bax/Bak oligomerization, releasing cytochrome c, which binds Apaf-1 to activate caspase-9 and initiate caspase-3-mediated apoptotic cascades. The extrinsic pathway involves Fas ligand binding to Fas receptors, recruiting FADD and activating caspase-8, which subsequently activates caspase-3. The balance between pro-apoptotic (Bax, Bak) and anti-apoptotic (Bcl2, BclXL) proteins determines cell fate (70). Renal I/R injury alters the Bax/Bcl2 ratio in the kidneys of humans, mice, and rats (71-73), resulting in an increase in Bax and a decrease in Bcl2. Wei Q *et al.* (74) used Bax- or Bak-knockout mice to demonstrate the important role of Bax and Bak in the apoptosis of renal tubular epithelial cells in ischemic AKI, suggesting that Bax or Bak gene knockout in proximal tubules can protect mice from ischemic AKI. Caspase-3, the central executioner of apoptosis, disrupts the cytoskeleton by cleaving actin filaments, impairing intracellular transport and signaling, and thus leading to cell death (75, 76). Our *in*

vitro H/R model confirmed increased HK-2 cell apoptosis post-H/R, which was mitigated by COR pretreatment. COR reversed H/R-induced expression of cleaved-Caspase3, Bax, and Bcl2, indicating its anti-apoptotic role in renal protection.

Necroptosis, a RIP kinase-regulated programmed necrosis, combines features of necrosis and apoptosis, manifesting as organelle swelling and membrane rupture (16, 77). Triggers include TNF family ligands, pathogen recognition receptors, oxidative stress, and interferons, with RIPK1, RIPK3, and MLKL as core mediators (78). Studies report elevated levels of necroptosis markers (RIPK1, RIPK3, MLKL) in H/R-induced HK-2 cells and in renal I/R models, alongside oxidative stress, inflammation, and renal dysfunction (79, 80). Our *in vitro* findings showed up-regulated RIPK1, RIPK3, MLKL, and p-MLKL in H/R-induced HK-2 cells, which were suppressed by COR pretreatment. Immunofluorescence confirmed reduced p-MLKL intensity in COR-treated cells. *In vivo*, I/R-induced AKI mice exhibited elevated serum creatinine and urea nitrogen, and elevated expression of KIM-1, NGAL, and renal p-MLKL, alongside severe tubular injury, as determined by HE staining. COR alleviated these markers, demonstrating its anti-necroptotic role in renal protection.

The 7-day prophylactic pre-treatment schedule adopted in this study has important clinical translational value: it is fully consistent with the 3-7-day preoperative preparation window for elective major surgery with high AKI risk in clinical practice, providing a feasible preventive strategy for these high-risk populations. Meanwhile, this design is a modern scientific verification of the traditional renal protective application of *C. militaris* through continuous pre-intervention, which provides rigorous preclinical evidence for the clinical transformation of this medicinal and edible fungus.

Accumulating evidence has demonstrated that the pathological process of renal ischemia-reperfusion injury is co-mediated by multiple programmed cell death pathways and inflammatory response, with extensive crosstalk between necroptosis, apoptosis, pyroptosis, and inflammatory signaling cascades. In this study, we confirmed that COR pre-treatment partially protects against I/R-induced AKI by regulating RIPK1-mediated necroptosis. Meanwhile, our results confirmed that COR can regulate the expression of the apoptosis-related proteins Bcl-2 and Bax, indicating that the anti-apoptotic effect is an important component of COR's renal protective mechanism. However, the specific regulatory pattern and underlying mechanism of the inflammatory response during COR that alleviates AKI by inhibiting apoptosis and necroptosis still need to be further explored in subsequent systematic studies. Another limitation of this study is that no prospective formal sample size power calculation was performed for the *in vivo* mouse experiments before study initiation. The sample size of n=6 mice per group was set based on the widely accepted convention and standard of preclinical AKI intervention studies. A formal power-calculation-based sample-size design will be strictly implemented in our subsequent preclinical validation studies to further enhance the statistical rigor of the research.

Conclusion

Using network pharmacology, our study identified 28 COR targets for the treatment of I/R-induced AKI, including Mapk1, Casp3, and Nfkb1, which are involved in biological processes and pathways such as apoptosis and necroptosis. In addition, *in vitro* experiments have shown that COR has antiapoptotic activity by restoring Bax/Bcl2 balance and inhibiting caspase-3 activation in H/R damaged renal tubular cells. *In vitro* experiments showed that COR can inhibit necroptosis by down-regulating RIPK1, RIPK3, MLKL, and p-MLKL in H/R-damaged HK-2 cells, confirming the role of COR in inhibiting RIPK1-driven necroptosis. *In vivo* experiments showed that COR can reduce the expression levels of kidney injury biomarkers (serum creatinine, urea nitrogen, KIM-1, NGAL), reduce the expression of p-MLKL associated with necroptosis, and improve kidney histopathological injury in I/R-induced AKI mice. In conclusion, our study combined network pharmacology and *in vivo*/*in vitro* experiments to clarify that COR partially protects I/R-induced AKI by regulating RIPK1-mediated necroptosis (shown in Figure 6).

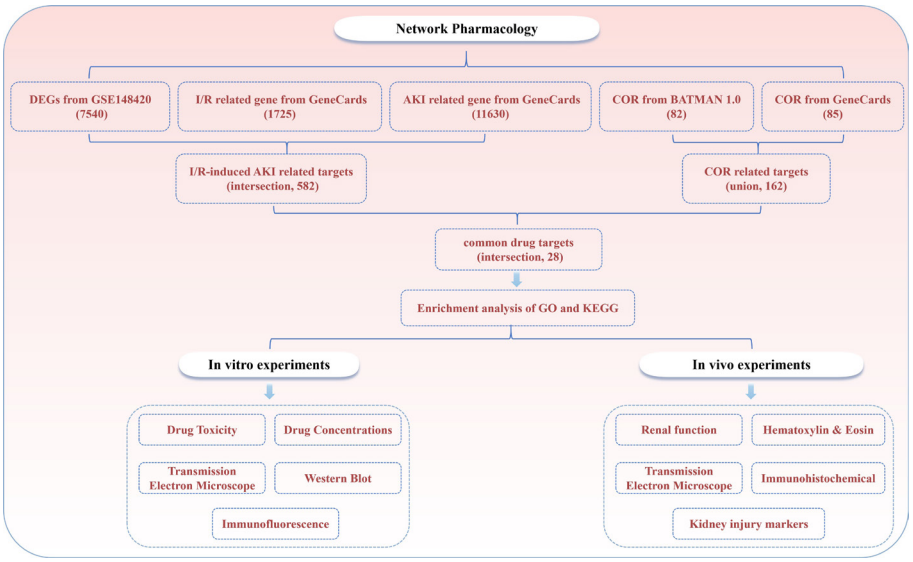

Figure 6. Schematic representation of COR ameliorating I/R-induced AKI by regulating RIPK1-mediated necroptosis
COR: Cordycepin; I/R: Ischemia/reperfusion; AKI: Acute kidney injury

Acknowledgment

We thank the reviewers and editors for their valuable comments and suggestions on this manuscript.

Statement of Ethics

This animal study was approved by the Shanxi Provincial People's Hospital animal ethics committee (approval: 2024-551).

Funding Sources

This research was funded by the Youth Scientific Research Project of the Basic Research Program of Shanxi Provincial Science and Technology Department (202403021222410), the Project of Shanxi Traditional Chinese Medicine Administration of Shanxi Provincial Health Commission (2023ZYYB029), and the Local Science and Technology Development Funds Projects Guided by Central Goverment (YDZJSX2025B007).

Data Availability Statement

The original dataset GSE148420 was obtained from the NCBI GEO database, and other processed data can be obtained from the corresponding author and supervision. The final draft was read and approved by all authors.

Authors' Contributions

XZ F and XT H designed the study and drafted the manuscript. ZB Z and JU L contributed to material preparation and data collection. SS T and F Z contributed to manuscript editing and formal analysis; XS Z was responsible for project administration and supervision. All authors read and approved the final draft.

Conflicts of Interest

The authors have no conflicts of interest to declare.

Declaration

We have not used any AI tools or technologies to prepare this manuscript.

References

1. Lameire NH, Levin A, Kellum JA, Cheung M, Jadoul M, Winkelmayer WC, *et al.* Harmonizing acute and chronic kidney disease definition and classification: Report of a Kidney Disease: Improving global outcomes (KDIGO) consensus conference. Kidney Int 2021; 100: 516-526.
2. Pérez-Aizpurua X, Cabello Benavente R, Bueno Serrano G, Peral JMA, Mañas BGJ, Jaumot JTI, *et al.* Obstructive uropathy: Overview of the pathogenesis, etiology and management of a prevalent cause of acute kidney injury. World J Nephrol 2024; 13: 93322.
3. Xu X, Nie S, Liu Z, Chen Ch, Xu G, Zha Y, *et al.* Epidemiology and Clinical Correlates of AKI in Chinese Hospitalized Adults. Clin J Am Soc Nephrol 2015; 10: 1510-1518.
4. Muiru AN, Hsu JY, Zhang X, Appel LJ, Chen J, Cohen DL, *et al.* Risk for chronic kidney disease progression after acute kidney injury: Findings from the chronic renal insufficiency cohort study. Ann Intern Med 2023; 176: 961-968.
5. Zhu Z, Hu J, Chen Z, Feng J, Yang X, Liang W, *et al.* Transition of acute kidney injury to chronic kidney disease: role of metabolic reprogramming. Metabolism 2022; 131:155194.
6. Allinson CS, Pollock CA, Chen X. Mesenchymal stem cells in the treatment of acute kidney injury (AKI), chronic kidney disease (CKD) and the AKI-to-CKD transition. Integr Med Nephrol Androl 2023; 10: e00014.
7. Hoste EAJ, Kellum JA, Selby NM, Zarbock A, Palevsky PM, Bagshaw SM, *et al.* Global epidemiology and outcomes of acute kidney injury. Nat Rev Nephrol 2018; 14: 607-625.
8. Ma FY, Tesch GH, Grynberg K, Ozols E, Mulley WR, Nikolic-Paterson DJ. A model of ischaemia-induced renal interstitial fibrosis in mice with established diabetes. Integr Med Nephrol Androl 2023; 10: e00032.
9. Zhang M, Liu Q, Meng H, Duan H, Liu X, Wu J, *et al.* Ischemia-reperfusion injury: Molecular mechanisms and therapeutic targets. Signal Transduct Target Ther 2024; 9: 12.
10. Mehta RL, Cerdá J, Burdmann EA, Tonelli M, García-García G, Jha V, *et al.* International society of nephrology's 0by25 initiative for acute kidney injury (zero preventable deaths by 2025): A human rights case for nephrology. Lancet 2015; 385: 2616-2643.
11. Havasi A, Borkan SC. Apoptosis and acute kidney injury. Kidney Int 2011; 80: 29-40.
12. He XY, Wang F, Suo XG, Gu MZ, Wang JN, Xu CH, *et al.* Compound-42 alleviates acute kidney injury by targeting RIPK3-mediated necroptosis. Br J Pharmacol 2023; 180: 2641-2660.
13. Chen Y, Wu MF, Xie MM, Lu Y, Li C, Xie SS, *et al.* Cpd-A1 alleviates acute kidney injury by inhibiting ferroptosis. Acta Pharmacol Sin 2024; 45: 1673-1685.
14. Chen Z, Li Y, Yuan Y, Lan K, Ye K, Lin Y, *et al.* Single-cell sequencing reveals homogeneity and heterogeneity of the cytopathological mechanisms in different etiology-induced AKI. Cell Death Dis 2023; 14:318.
15. Xiang T, Li L-Z, Li J, Chen X-Y, Guo F, Liu J, *et al.* Chromodomain Y-like (CDYL) inhibition ameliorates acute kidney injury in mice by regulating tubular pyroptosis. Acta Pharmacol Sin 2024; 45: 2598–2610.
16. Kolbrink B, von Samson-Himmelstjerna FA, Murphy JM, Krautwald S. Role of necroptosis in kidney health and disease. Nat Rev Nephrol 2023; 19: 300–314.
17. Galluzzi L, Kepp O, Chan FK-M, Kroemer G. Necroptosis: Mechanisms and relevance to disease. Annu Rev Pathol 2017; 12: 103-30.
18. Pefanis A, Ierino FL, Murphy JM, Cowan PJ. Regulated necrosis in kidney ischemia-reperfusion injury. Kidney Int 2019; 96: 291–301.
19. Chen L, Deng Y, Hu J, Gong X. Nephroprotective effects of substances of medicine food homology and traditional Chinese medicine phytochemicals against acute kidney injury. Front Pharmacol 2025; 16: 1539886.
20. Huang J, Liang Y, Zhou L. Natural products for kidney disease treatment: Focus on targeting mitochondrial dysfunction. Front Pharmacol 2023; 14: 1142001.
21. Zhong X, Jia J, Tan R, Wang L. Hederagenin improves adriamycin-induced nephropathy by inhibiting the JAK/STAT signaling pathway. Integr Med Nephrol Androl 2024; 11: e22-00016.
22. Wang YN, Li XJ, Wang WF, Zou L, Miao H, Zhao YY. Geniposidic acid attenuates chronic tubulointerstitial nephropathy through regulation of the NF-ƙB/Nrf2 pathway via aryl hydrocarbon receptor signaling. Phytother Res 2024; 38: 5441–5457.
23. Zeng J, Zhou Y, Lyu M, Huang X, Xie M, Huang M, *et al.* Cordyceps militaris: A novel mushroom platform for metabolic engineering. Biotechnol Adv 2024; 74: 108396.
24. Nxumalo W, Elateeq AA, Sun Y. Can cordyceps cicadae be used as an alternative to cordyceps militaris and cordyceps sinensis? A review. J Ethnopharmacol 2020; 257: 112879.
25. Dong C, Guo S, Wang W, Liu X. Cordyceps industry in China. Mycology 2015; 6: 121–129.
26. Yang L, Li G, Chai Z, Gong Q, Guo J. Synthesis of cordycepin: Current scenario and future perspectives. Fungal Genet Biol 2020; 143: 103431.
27. Reis FS, Barros L, Calhelha RC, Cirić A, van Griensven LJLD, Soković M, *et al.* The methanolic extract of Cordyceps militaris (L.) Link fruiting body shows antioxidant, antibacterial, antifungal and antihuman tumor cell lines properties. Food Chem Toxicol 2013; 62: 91–98.

28. Yu S-H, Dubey NK, Li W-S, Liu M-C, Chiang H-S, Leu S-J, *et al.* Cordyceps militaris treatment preserves renal function in type 2 diabetic nephropathy mice. PLoS One 2016; 11: e0166342.
29. Yang C-H, Kuo W-S, Wang J-S, Hsiang Y-P, Lin Y-M, Wang YT, *et al.* Improvement in the blood urea nitrogen and serum creatinine using new cultivation of cordyceps militaris. Evid Based Complement Alternat Med 2022; 2022: 4321298.
30. Cunningham KG, Manson W, Spring FS, Hutchinson SA. Cordycepin, a metabolic product isolated from cultures of *Cordyceps militaris* (Linn.) Link. Nature 1950; 166: 949.
31. Aydogdu B, Basuguy E, Arslan S, Azizoğlu M, Ibiloglu İ, Kaplan İ, *et al.* The effect of low-dose Cordyceps on ischemia-reperfusion injury of the kidney in rats. Cir Cir 2022; 90: 69–74.
32. Tang Z and Zhu Y. Cordycepin ameliorates kidney injury by inhibiting gasdermin D-mediated pyroptosis of renal macrophages through nuclear factor kappa-B. J Biochem Mol Toxicol 2024; 38: e23824.
33. Ashraf SA, Elkhalifa AEO, Siddiqui AJ, Patel M, Awadelkareem AM, Snoussi M, *et al.* Cordycepin for health and wellbeing: a potent bioactive metabolite of an entomopathogenic cordyceps medicinal fungus and its nutraceutical and therapeutic potential. Molecules 2020; 25: 2735.
34. Jin Y, Meng X, Qiu Z, Su Y, Yu P, Qu P. Anti-tumor and anti-metastatic roles of cordycepin, one bioactive compound of Cordyceps militaris. Saudi J Biol Sci 2018; 25: 991–995.
35. Yue K, Ye M, Zhou Z, Sun W, and Lin X. The genus Cordyceps: A chemical and pharmacological review. J Pharm Pharmacol 2013; 65: 474–493.
36. Sun Y, Jin S, Chen J, Zhang J, Lu Y, Gu Q, *et al.* Cordycepin ameliorates renal interstitial fibrosis by inhibiting Drp1-mediated mitochondrial fission. Drug Des Devel Ther 2025; 19: 1271-1287.
37. Chen Q, Guo J, Han S, Wang T, Xia K, Yu B, *et al.* Cordycepin alleviates renal ischemia-reperfusion injury by suppressing the p38/JNK signaling pathway. Int Immunopharmacol 2025; 150: 114264.
38. Gu L, Johno H, Nakajima S, Kato H, Takahashi S, Katoh R, *et al.* Blockade of Smad signaling by 3'-deoxyadenosine: A mechanism for its anti-fibrotic potential. Lab Invest 2013; 93: 450–461.
39. Kellum JA, Romagnani P, Ashuntantang G, Ronco C, Zarbock A, Anders H-J. Acute kidney injury. Nat Rev Dis Primers 2021; 7: 52.
40. Lathiya MK, Errabelli P, Roy S, Mareedu N. Severe acute kidney injury due to oxalate crystal induced severe interstitial nephritis: A case report. World J Nephrol 2024; 13: 93976.
41. Du Y, Li J, Ye M, Guo C, Yuan B, Li S, *et al.* Hyperuricemia-induced acute kidney injury in the context of chronic kidney disease: A case report. Integr Med Nephrol Androl 2023; 10: e00008.
42. Fu Y, Dong Z. Immune response in COVID-19-associated acute kidney injury and maladaptive kidney repair. Integr Med Nephrol Androl 2023; 10: e00022.
43. Huang MJ, Ji YW, Chen JW, Li D, Zhou T, Qi P, *et al.* Targeted VEGFA therapy in regulating early acute kidney injury and late fibrosis. Acta Pharmacol Sin 2023; 44: 1815–1825.
44. Jiang L, Sun XY, Wang SQ, Liu YL, Lu LJ, Wu W-H, *et al.* Indoxyl sulphate-TNFα axis mediates uremic encephalopathy in rodent acute kidney injury. Acta Pharmacol Sin 2024; 45: 1406–1424.
45. Li X-L, Liu X-W, Liu W-L, Lin Y-Q, Liu J, Peng Y-S, *et al.* Inhibition of TMEM16A improves cisplatin-induced acute kidney injury via preventing DRP1-mediated mitochondrial fission. Acta Pharmacol Sin 2023; 44: 2230–2242.
46. Cao F, Li Y, Peng T, Li Y, Yang L, Hu L, *et al.* PTEN in kidney diseases: A potential therapeutic target in preventing AKI-to-CKD transition. Front Med (Lausanne) 2024; 11: 1428995.
47. Kim M-G, Cho WY, Chung SM, Choi YE, Fang Y, Park MS, *et al.* Altered gut microbiome plays an important role in AKI to CKD transition in aged mice. Front Med (Lausanne) 2023; 10: 1238960.
48. Song Z, Gong X. Research Progress on the Potential mechanisms of acute kidney injury and chronic kidney disease induced by proton pump inhibitors. Integr Med Nephrol Androl 2023; 10: e00027.
49. Li X-J, Suo P, Wang Y-N, Zou L, Nie X-L, Zhao Y-Y, *et al.* Arachidonic acid metabolism as a therapeutic target in AKI-to-CKD transition. Front Pharmacol 2024; 15: 1365802.
50. Wang F, Zhou L, Eliaz A, Hu C, Qiang X, Ke L, *et al.* The potential roles of galectin-3 in AKI and CKD. Front Physiol 2023; 14: 1090724.
51. Sanz AB, Sanchez-Niño MD, Ramos AM, Ortiz A. Regulated cell death pathways in kidney disease. Nat Rev Nephrol 2023; 19: 281–299.
52. Li Y, Min X, Zhang X, Cao X, Kong Q, Mao Q, *et al.* HSPA12A promotes c-Myc lactylation-mediated proliferation of tubular epithelial cells to facilitate renal functional recovery from kidney ischemia/reperfusion injury. Cell Mol Life Sci 2024; 81: 404.
53. Zhang HW, Lin ZX, Tung YS, Kwan TH, Mok CK, Leung C, *et al. Cordyceps sinensis* (a traditional Chinese medicine) for treating chronic kidney disease. Cochrane Database Syst Rev 2014; 2014: CD008353.
54. Wang Y-N, Zhang Z-H, Liu H-J, Guo Z-Y, Zou L, Zhang Y-M, *et al.* Integrative phosphatidylcholine metabolism through phospholipase A2 in rats with chronic kidney disease. Acta Pharmacol Sin 2023; 44: 393–403.
55. Liu Q, Li X, Pan Y, Liu D, Li Y, He C, *et al.* Efficacy and safety of Qushi Huayu, a traditional Chinese medicine, in patients with nonalcoholic fatty liver disease in a randomized controlled trial. Phytomedicine 2024; 130: 155398.
56. Wu J, Tang G, Zheng C-S, Yeerken R, Chan Y-T, Fu Z, *et al.* Traditional Chinese medicine for the treatment of cancers of hepatobiliary system: From clinical evidence to drug discovery. Mol Cancer 2024; 23: 218.
57. Yang Y, Li X, Chen G, Xian Y, Zhang H, Wu Y, *et al.* Traditional chinese medicine compound (tongxinluo) and clinical outcomes of patients with acute myocardial infarction: The CTS-AMI randomized clinical trial. JAMA 2023; 330: 1534–1545.
58. Cheang I, Yao W, Zhou Y, Zhu X, Ni G, Lu X, *et al.* The traditional Chinese medicine Qiliqiangxin in heart failure with reduced ejection fraction: A randomized, double-blind, placebo-controlled trial. Nat Med 2024; 30: 2295–2302.
59. Zhao B-R, Hu X-R, Wang W-D, Zhou Y. Cardiorenal syndrome: Clinical diagnosis, molecular mechanisms and therapeutic strategies. Acta Pharmacol Sin 2025; 46: 1539–1555.
60. Guo J, Chen X, Wu M, Wang D, Zhao Y, Li Q, *et al.* Traditional Chinese medicine FYTF-919 (Zhongfeng Xingnao oral prescription) for the treatment of acute intracerebral haemorrhage: A multicentre, randomised, placebo-controlled, double-blind, clinical trial. Lancet 2024; 404: 2187-2196.
61. Li Z, Ludwig N, Thomas K, Mersmann S, Lehmann M, Vestweber D, *et al.* The pathogenesis of ischemia-reperfusion induced acute kidney injury depends on renal neutrophil recruitment whereas sepsis-induced AKI does not. Front Immunol 2022; 13: 843782.
62. Guo Z-Y, Wu X, Zhang S-J, Yang J-H, Miao H, Zhao Y-Y. Poria cocos: Traditional uses, triterpenoid components and their renoprotective pharmacology. Acta Pharmacol Sin 2025; 46: 836-851.
63. Liu D, Tang S, Gan L, Cui W. Renal-protective effects and potential mechanisms of traditional chinese medicine after ischemia-reperfusion injury. Evid Based Complement Alternat Med 2021; 2021: 5579327.
64. Cao G, Miao H, Wang Y-N, Chen D-Q, Wu X-Q, Chen L, *et al.* Intrarenal 1-methoxypyrene, an aryl hydrocarbon receptor agonist, mediates progressive tubulointerstitial fibrosis in mice. Acta Pharmacol Sin 2022; 43: 2929–2945.
65. Xiao L, Ge Y, Sun L, Xu X, Xie P, Zhan M, *et al.* Cordycepin inhibits albumin-induced epithelial-mesenchymal transition of renal tubular epithelial cells by reducing reactive oxygen species production. Free Radic Res 2012; 46: 174-183.
66. Han F, Dou M, Wang Y, Xu C, Li Y, Ding X, *et al.* Cordycepin protects renal ischemia/reperfusion injury through regulating inflammation, apoptosis, and oxidative stress. Acta Biochim Biophys Sin (Shanghai) 2020; 52: 125–132.
67. Okur MH, Arslan S, Aydogdu B, Zeytun H, Basuguy E, Arslan

MS, *et al*. Protective effect of cordycepin on experimental testicular ischemia/reperfusion injury in rats. J Invest Surg 2018; 31: 1-8.
68. Wang Y, Xi W, Zhang X, Bi X, Liu B, Zheng X, *et al*. CTSB promotes sepsis-induced acute kidney injury through activating mitochondrial apoptosis pathway. Front Immunol 2022; 13: 1053754.
69. Lv W, Liao J, Li C, Liu D, Luo X, Diao R, *et al*. Aquaporin 1 is renoprotective in septic acute kidney injury by attenuating inflammation, apoptosis and fibrosis through inhibition of P53 expression. Front Immunol 2024; 15: 1443108.
70. Lossi L. The concept of intrinsic versus extrinsic apoptosis. Biochem J 2022; 479: 357-384.
71. Wolfs TGAM, de Vries B, Walter SJ, Peutz-Kootstra CJ, van Heurn LWE, Oosterhof GON, *et al*. Apoptotic cell death is initiated during normothermic ischemia in human kidneys. Am J Transplant 2005; 5: 68–75.
72. Han SJ, Jang H-S, Noh MR, Kim J, Kong MJ, Kim JI, *et al*. Mitochondrial NADP+-dependent isocitrate dehydrogenase deficiency exacerbates mitochondrial and cell damage after kidney ischemia-reperfusion injury. J Am Soc Nephrol 2017; 28: 1200-1215.
73. Shen S, Zhou J, Meng S, Wu J, Ma J, Zhu C, *et al*. The protective effects of ischemic preconditioning on rats with renal ischemia-reperfusion injury and the effects on the expression of Bcl-2 and Bax. Exp Ther Med 2017; 14: 4077-4082.
74. Wei Q, Dong G, Chen J-K, Ramesh G, Dong Z. Bax and Bak have critical roles in ischemic acute kidney injury in global and proximal tubule-specific knockout mouse models. Kidney Int 2013; 84: 138-148.
75. Larsen BD, Sørensen CS. The caspase-activated DNase: Apoptosis and beyond. FEBS J 2017; 284: 1160–1170.
76. Liang Y, Liu Z, Qu L, Wang Y, Zhou Y, Liang L, *et al*. Inhibition of the IRE1/JNK pathway in renal tubular epithelial cells attenuates ferroptosis in acute kidney injury. Front Pharmacol 2022; 13: 927641.
77. Alassaf N, Attia H. Autophagy and necroptosis in cisplatin-induced acute kidney injury: Recent advances regarding their role and therapeutic potential. Front Pharmacol 2023; 14: 1103062.
78. Yuan J and Ofengeim D. A guide to cell death pathways. Nat Rev Mol Cell Biol 2024; 25: 379–395.
79. He X-Y, Wang F, Suo X-G, Gu M-Z, Wang J-N, Xu C-H, *et al*. Compound-42 alleviates acute kidney injury by targeting RIPK3-mediated necroptosis. Br J Pharmacol 2023; 180: 2641–2660.
80. Shiva N, Sharma N, Kulkarni YA, Mulay SR, Gaikwad AB. Renal ischemia/reperfusion injury: An insight on *in vitro* and *in vivo* models. Life Sci 2020; 256: 117860.